Revista
GEOCIÊNCIAS

ISSN: 1980-900X (online)

ESTIMATING THE UNCERTAINTY OF KRIGING ESTIMATES: A PRACTICAL REVIEW AND THE PROPOSAL OF TWO NOVEL-APPROACHES

ESTIMANDO A INCERTEZA DAS ESTIMATIVAS DE KRIGAGEM: UMA REVISÃO PRÁTICA E A PROPOSTA DE DUAS NOVAS ABORDAGENS

Victor MIGUEL SILVA

Gerência de Padronização e Integração (COI Planejamento), VALE - Av. Dr. Marco Paulo Simon Jardim, 3580 - Vila da Serra, Nova Lima – MG. E-mail: victormiguelsilva@hotmail.com

Introduction
Review of Methods
Kriging Variance (KV)
Interpolation Variance (IV)
Indicator Kriging (IK)
Combined Variance (CV)
Median IK (mIK)
Multi-Gaussian Kriging (mGK)
Methodology
The Combined Variance II
The Combined Index (CI)
Combined Index: an illustrative example
Comparative example
Presentation of the dataset
Measuring the model uncertainty
Discussions and conclusions
References

RESUMO - Este artigo apresenta dois novos métodos baseados em krigagem para medir a incerteza associada às estimativas. Ambas as abordagens combinam a Variância de Krigagem (KV), que é um bom índice da configuração espacial dos dados, com uma segunda componente que mede localmente a dispersão dos dados. O primeiro método proposto, denominado Índice Combinado (IC), mescla o KV com a distribuição condicional local estimada por *Median Indicator Kriging*. O nome do segundo método proposta é Variância Combinada II (CVII), altera a equação originalmente proposta pela "Variância Combinada" para combinar KV e a Variância de Interpolação. No estudo de caso, comparamos os dois métodos propostos com outras abordagens disponíveis na literatura usando o amplamente conhecido conjunto de dados de Walker Lake. Os resultados indicam que ambos os métodos propostos superaram as demais soluções disponíveis. O índice CVII superou sua formulação original em todos os cenários testados.
Palavras-Chave: Geoestatística. Incerteza da Krigagem. Median Indicator Kriging. Variância de interpolação.

ABSTRACT - This paper presents two novel kriging-based methods to measure the uncertainty associated with geostatistical estimates. Both approaches combine the Kriging Variance (KV), which is a good summary of the spatial configuration of the data, with a second component which locally measures the data dispersion. The first proposed method, referred to as the Combined Index (CI), merges KV with the local conditional distribution estimated by median Indicator Kriging. The name of the other method is Combined Variance II (CVII) revises the equation originally proposed by Combined Variance to merge KV and the Interpolation Variance. We compare the two proposed methods to other approaches available in the literature in a case study using the widely known Walker Lake dataset. The results indicate that both proposed methods outperformed the other tested solutions. The CVII index outperformed its original formulation in all the tested scenarios.
Keywords: Geostatistics. Kriging Uncertainty. Median Indicator Kriging. Interpolation Variance.

INTRODUCTION

All models are subject to uncertainty and no analysis or decision-making is optimal if we ignore this fact. Therefore, it is highly recommended to associate an index of uncertainty to any estimated value.

The methods of geostatistical simulation, specifically the sequential methods, became in the last decades the standard approach to quantify uncertainties and classify the mineral resources (CIM, 2019; Gómez-Hernández & Srivastava, 2021). However, estimating the uncertainty by kriging-based methods still have some advantages:

- Kriging-based methods are computationally cheap, being adequate to almost any modelling routines. Simulating and processing a large number of realizations is a cumbersome process that may not fit to routines performed on a daily or weekly basis, such as grade control or short-term;

- Methods of simulation and estimation commonly relies on different assumptions and have different properties. The space of uncertainty assessed by geostatistical simulation may overlook or overweigh the real sources of deviation between the kriged and actual value. Example of possible factors are domain stationarity, conditional bias and sensibility to outlier, among others.

Considering the kriging-based methods available in the literature and their limitations, we propose two novel indexes of uncertainty: (i) The Combined Index which merges Kriging Variance (KV; Matheron, 1963) with the conditional cumulative distribution function (ccdf) locally estimated by median Indicator Kriging (IK; Journel, 1982); and (ii) the Combined Variance II (CVII), an adaptation of the method originally proposed by Arik (1999). CVII uses a new equation to merge KV and Interpolation Variance (IV; Yamamoto, 2000).

This paper is structured as follows: methods available in the literature and their properties are reviewed. It is presented both the novel proposed methods, referred to as Combined Index (CI) and Combined Variance II (CVII). Next, both proposed methods are applied to the Walker Lake data (Isaaks & Srivastava, 1989) and their results are compared with methods available in the literature. Discussions and conclusions follow.

REVIEW OF METHODS

The focus of the present section is to review geostatistical methods and relevant properties we will refer to it later in this article. For further details and fundamentals of the cited subject, the reader is directed to standard geostatistical textbooks (e.g. Journel & Huijbregts, 1978; lsaaks & Srivastava 1989; Goovaerts, 1997; Deutsch & Journel, 1998).

Kriging Variance (KV)

The KV has three key properties that are relevant in this study (Goovaerts, 1997): (i) it is dependent on the used variogram model, (ii) dependent on the data configuration on the space, and (iii) independent of data values. Goovaerts qualifies the first two properties as excellent features, but he considers the third property to be a bad feature because it results in the fact that an area surrounded by data with heterogeneous or homogeneous grades has the same KV (Figure 1).

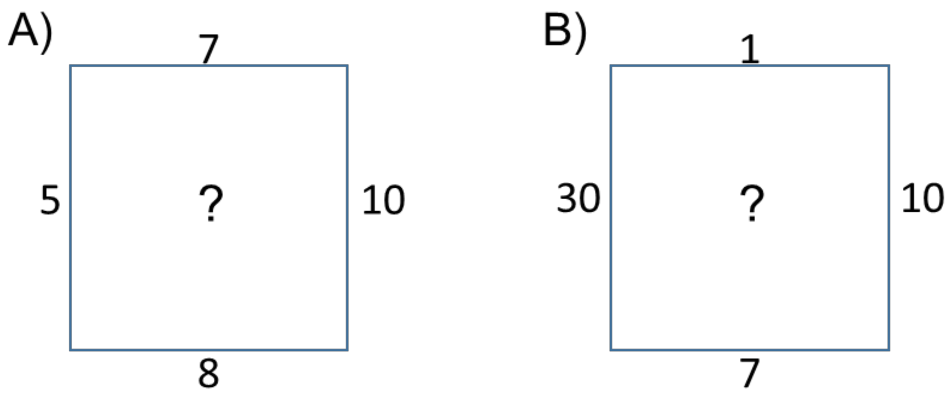

Figure 1 - Estimation of blocks from the same data configuration. The Kriging Variance of A and B is the same due to its independence do data values (Adapted from Armstrong 1984).

Therefore, we consider KV a good summary of the spatial configuration given the modelled variogram structural distance.

Hereafter KV will be respectively referred to as σ^2_{OK} or σ^2_{SK} when computed respectively from Ordinary (OK) or Simple Kriging (SK; Matheron, 1963).

Interpolation Variance (IV)

The IV measures the local data dispersion through the average difference between the estimated value $z^*(x_0)$ and its n retained data $z(x_i)$ weighted by the kriging weights w_i, where $i = 1,..,n$ (Equation 1).

$$\sigma^2_{IV} = \sum_{i=1}^{n} w_i [z(x_i) - z^*(x_0)]^2 \quad (1)$$

The variance σ^2_{IV} increases with the variability of $z(x_i)$ around x_0.

The IV is assumed as being indirectly influenced by the variogram structural distance associated with the weights w_i. More details in Yamamoto (2000).

Indicator Kriging (IK)

The IK (Journel, 1983) handle with transformed data within a chosen stationary domain, we code observations as 1 if their values are above a given threshold grade and otherwise, they are assigned to 0. The estimated indicators can be interpreted as the probability or proportion of each point to belong to the class defined by the threshold as 1. It is worth to highlight that IK estimates are dependent on the indicators variability, but little influenced by data spacing (Figure 2).

Combined Variance (CV)

The CV combines KV, which explicitly accounts for the local variability of the variable of interest and the IV, which is a good summary of the spatial data configuration around the estimated node (Equation 2).

$$\sigma^2_{CV} = \sqrt{\sigma^2_{IV} * \sigma^2_{OK}} \quad (2)$$

The use of non-normalized variogram to compute CV is necessary to assure that IV and KV are in the same scale (Arik, 1999).

Median IK (mIK)

We may use the mIK as a non-parametrical method to produce an approximation of the local distribution at each unsampled node thought discretizing the ccdf into multiple thresholds (Figure 3).

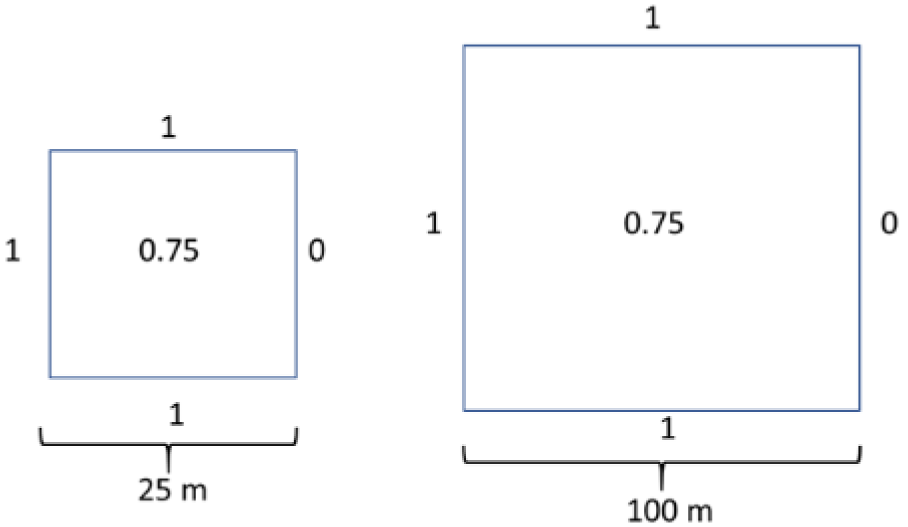

Figure 2 - Estimation of blocks from the same indicator values. See that both estimated values are equal, indifferently of the distance between data and the block node.

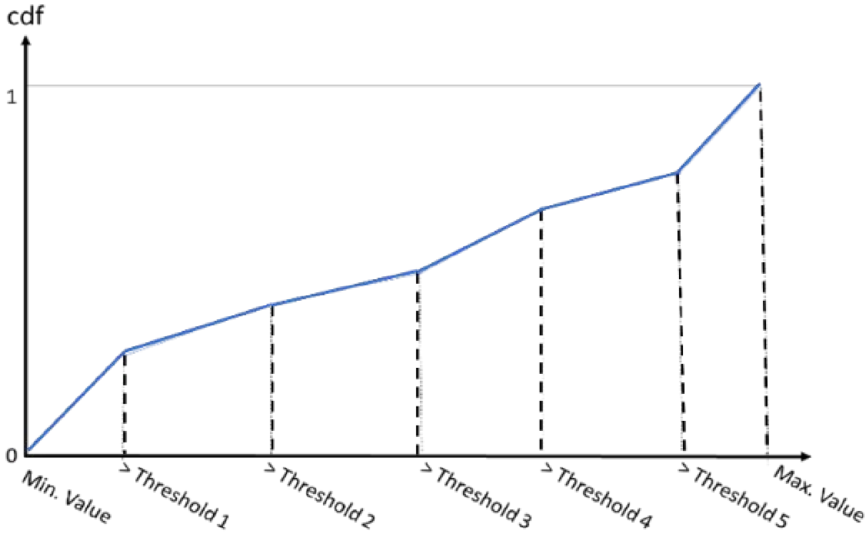

Figure 3 – Ccdf inferred by interpolating the probabilities between pairs of classes estimated by multiple Indicator Kriging. The tails are extrapolated by a defined equation between the lower threshold and the minimum value, and between the upper threshold and the maximum value.

The median IK simplifies the task of managing several thresholds by assuming that we can approximate the individual variogram for each class K by a single model, usually, the indicator variogram of the median. We highlight the following points of attention:

(i) The assumption that we may approximate each K variogram by a single model always must be checked (Isaaks & Srivastava, 1989, pp. 444). Other solutions to manage multiple classes must be considered when the median IK assumption does not hold;

(ii) The mIK estimates are very sensitive to the assumption of stationarity. It is recommended analyzing whether the defined thresholds are both locally and globally adequate to all domain areas;

(iii) The estimates are carried out separately for each class K, and then the order relations of the resulting estimated ccdf values must corrected if necessary (Journel, 1983; Deutsch and Journel, 1998). We recommend discretizing the data distribution into a number between 7 and 15 classes.

Journel (1983), Deutsch & Journel (1998) or Carvalho & Deutsch (2017) presents more details about IK, median IK and estimating ccdf from multiple thresholds;

Multi-Gaussian Kriging (mGK)

The mGK relies on the property in which any weighted average of multi-Gaussian variables follows the same distribution, and that these distributions may be entirely determined by the value and variance computed by Simple Kriging, in which relies on a strong assumption of stationarity (Verly, 1983, 2005; Deutsch & Journel, 1998). As most variables are not Gaussian, the approach requires a quantile transformation of data value and a back transformation of the estimated values, a procedure called "normal-score transformation".

Next section presents two novel approaches, the CI is based on combining local ccdf estimated by median IK with σ^2_{OK} while CVII combines σ^2_{OK} with the Interpolation Variance.

METHODOLOGY

The Combined Variance II

The Combined Variance II (CVII) replaces the Equation 2 originally proposed by Arik (1999) by Equation 3, a theoretically sound equation to combine distributions. In the independent case we get:

$$\text{CVII} = \sqrt{\sigma^2_{ok}\sigma^2_{IV} + \bar{z}^2_{ok}(\sigma^2_{IV} + \sigma^2_{ok})} \quad (3)$$

In the dependent case, it is necessary to use Equation (4) in its full form. It is always recommended to check the hypothesis that the dependence is negligible because this relationship may occur as stated in Yamamoto (2000): "*[…] the interpolation variance indirectly uses the variogram structural distance through the ordinary kriging weight. The more influential datum location receives the greater weight.*"

The Combined Index (CI)

The CI combines the Kriging Variance σ^2_{ok} with the variance σ^{*2}_{ccdf} of the ccdf estimated by median IK through equation 4, which shows the product of two distributions (X and Y) in the dependent case:

$$\sigma^2(X{*}Y) = \text{Cov}(X^2,Y^2)+[\sigma^2(X)+E(X)^2]\cdot[\sigma^2(Y)+E(Y)^2]-[\text{Cov}(X,Y)+E(X)E(Y)]^2 \quad (4)$$

Note that in the independent case $\text{Cov}(X^2, Y^2) = 0$ the terms $[E(X)E(Y)]^2$ cancel out. Under the assumption of independence between σ^2_{ok} and σ^{*2}_{ccdf}, the proposed index is defined as follows (Equation 5):

$$\sigma^2_{CI} = \text{CI} = \sqrt{\sigma^2_{ok}\sigma^2_{cdf} + \bar{z}^2_{ok}\sigma^2_{cdf} + \bar{z}^2_{mIK}\sigma^2_{ok}} \quad (5)$$

The CI has the following features: (i) The index is zero if the estimated node coincides with a sampled datum; (ii) The KV component makes it a good index of the data configuration, being proportional to the variogram structural distance; (iii) The σ^{*2}_{ccdf} component is proportional to the local data variability. The Kriging Variance must be computed considering the original-units variogram so that it would be on the same scale of the estimated ccdf. Next, we apply the Combined Index in one schematic case.

Combined Index: an illustrative example

The illustrative case study uses a synthetic bidimensional dataset of the continuous variable V. The data positions are randomly distributed in space following an average spacing of 200 x 200 m. The data values are a single realization drawn from a non-conditional simulation with a highly skewed distribution and an isotropic variogram model with a single spherical structure with a range of 800 m and variance contribution C = 15.000 (75%), and nugget C_0 = 5.000 (25%) (Figure 4a). A small area with 21 values was sampled from the simulated dataset. The subset is used to illustrate the CI index as a function of the values of four clustered values, referred to as X, Y, Z and K (Figure 4b).

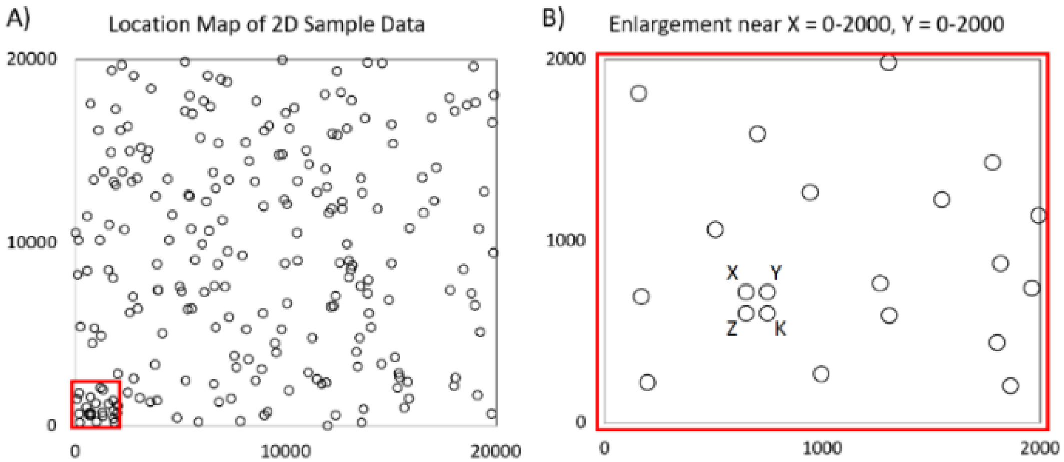

Figure 4 - A) map of the sample data and B) enlarged around the area to be analyzed.

The normalized median variogram of V is isotropic with range of 1100 m, C = 0.85, and C_0 = 0.15. All estimates required at least 10 data in the neighbourhood. The percentiles 0.15, 0.3, 0.45, 0.5, 0.6, 0.75, and 0.9 are respectively delimited by the grades 7, 11, 13, 14, 15, 28, and 52 units. The variogram models and the distribution of the variables of interest are assumed the same in all scenarios since the four varying values (X, Y, Z and K) correspond to less than 2% of the complete dataset.

The median IK and OK estimates were carried out using a non-discretized 5 x 5 m block model. Figure 5 shows the CI map of four scenarios. The available data are distributed over a wide range of values, the low-grades domain is preferentially located in the superior area (Vertical axis > 1600 m) and the high-grade in the central areas.

The samples X, Y, Z and K are in the transition between these domains. Each scenario attributes different values of V to samples X, Y, Z and K. The Ordinary Kriging Variance (Figure 5a) is the same in all scenarios.

In Figure 5b, we have in the first scenario the values X = Y = Z = K = 50 and the dashed area shows a high-grade domain with low uncertainty. The CI values rise towards NW, indicating a high uncertainty at the abrupt transition between the dashed area and the low-grade domain. In figure 4c, the values X = Y = Z = K = 5 reduces the high-grade domain and increase the index on the left side of the dashed-circle because of the abrupt change between areas. In figure 5d we have X = Z = 5 and Y = K = 50 while in Figure 5e X = Z = 70 and Y = K = 5, in both scenarios we observe an area with highly heterogeneous grades. Figure 5e shows a large CI indicating a high uncertainty about the limits between the different clusters of high and low values in a highly heterogeneous spatial distribution.

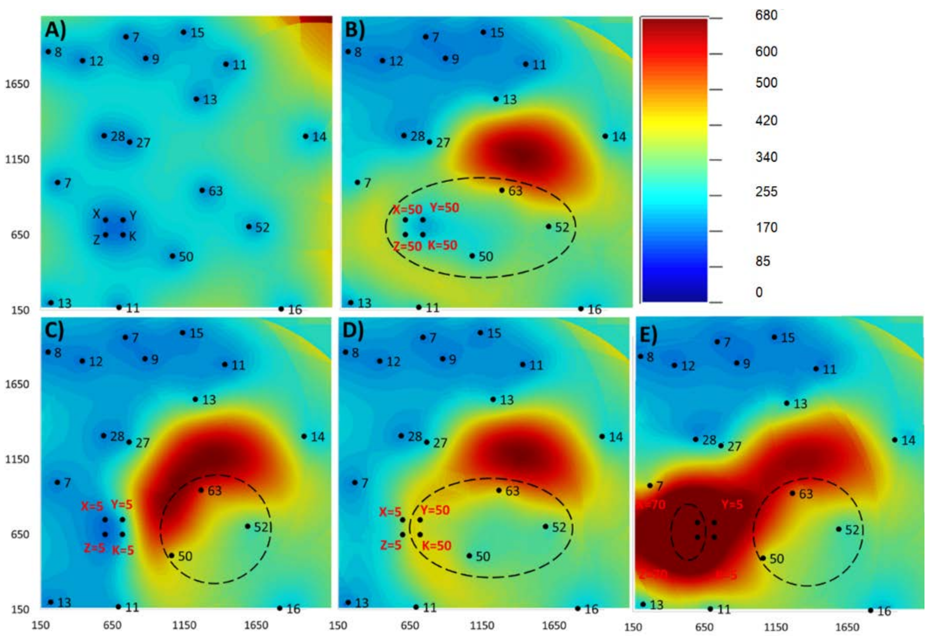

Figure 5 - Maps of the A) Kriging Variance of all scenarios and the individual maps of combined deviation of four scenarios with different values of the samples X, Y, Z and K. All maps plotted in standard deviation units.

Figure 6 shows a linear relationship of the scatterplots and the correlation coefficient ranging from 0.59 to 0.78 between the CI estimated uncertainty (x-axis) and the uncertainty simulated by Sequential Gaussian Simulation in the y-axis (Isaaks 1990; Deutsch & Journel 1998). The simulation of 100 realizations is carried out in 200 x 200 m blocks discretized in a 5 x 5 m grid.

We observe that the CI value is greater at the locations surrounded by data with heterogeneous values than at a location surrounded by data with similar values.

The bigger is the distance between the data and the estimated node, or more clustered the data are, the higher the CI value is. Next, both proposed methods are compared to other methods available in the literature.

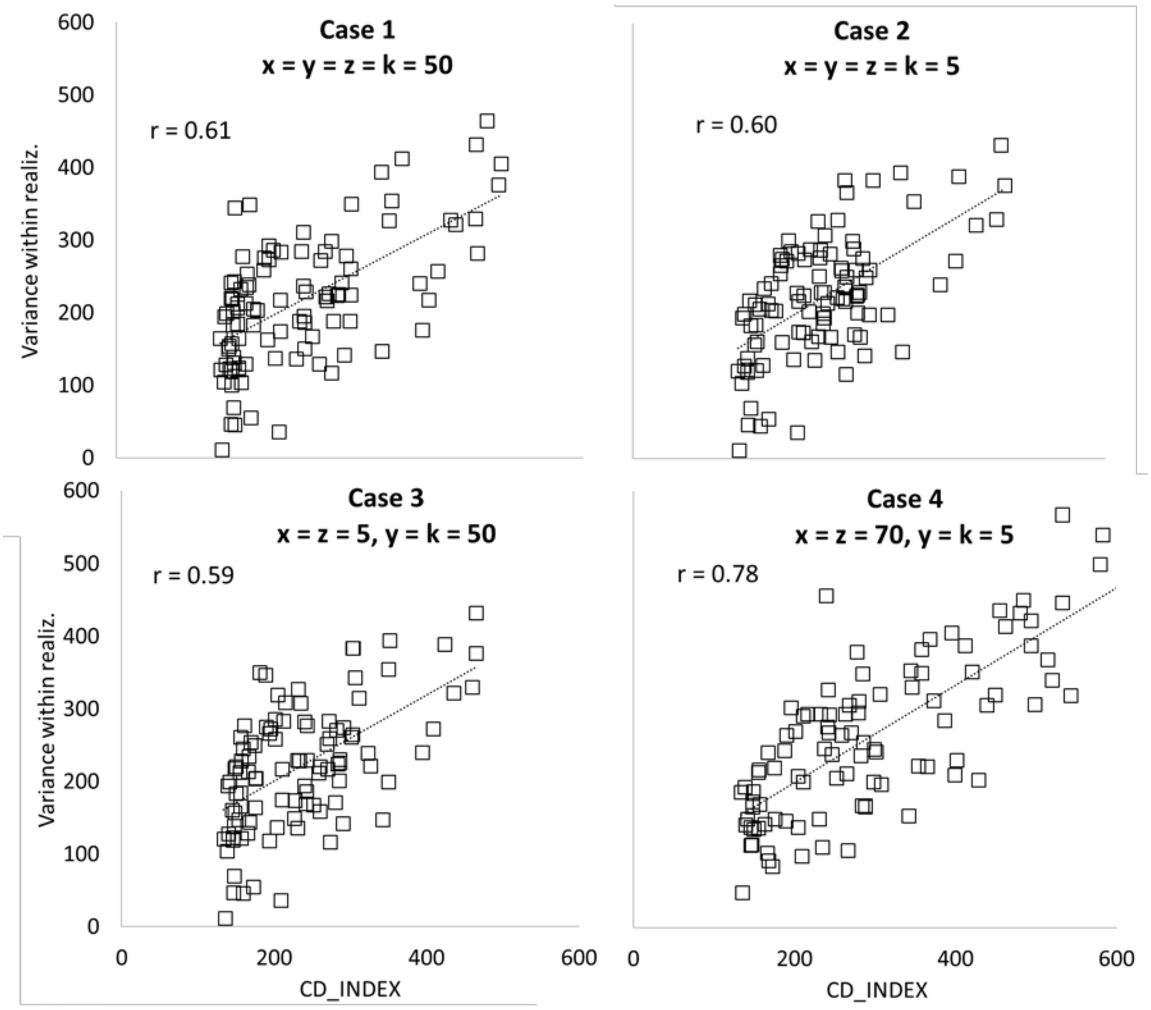

Figure 6 - Scatter plot between the Combined Deviation (x-axis) and the variance within realizations, both computed at 200 x 200 m blocks discretized in a 5 x 5 m grid. The four cases use the same dataset which variations on the values of samples X, Y, Z and K.

COMPARATIVE EXAMPLE

Presentation of the dataset

In this example the proposed and reviewed methods are applied to two re-scaled datasets of the exhaustive Walker Lake dataset (Isaaks & Srivastava, 1989). The first dataset is composed of 196 samples of the variable U in a pseudo-regular grid of 20 x 20 m. The second dataset is composed of 469 samples, combining the first dataset with additional data preferentially sampled in the high-grade areas.

The variogram models were adjusted for the exhaustive dataset in original units (8a), indicator of the median (8b) and for data in Normal-Score units (8c). All models showed anisotropy with longer and shorter continuity respectively in the N157.5° and N67.5º directions. We used Ordinary Kriging for estimate in 10 x 10 m blocks the U variable of both re-scaled datasets (Figure 7b and 7c). All methods were run using the open-source software SGeMS (Remy, 2009), Datamine® Studio RM® 1.9 and algorithms wirtten by the author. However, it is worth to highlight that the presented algorithms may be run in almost any geostatistical software with minor adaptations.

The search ellipse ranges are equal to the range of the original-units variogram (Figure 8), with a minimum of 12 and a maximum of 48 samples. All negative weights were reset to zero and the sum of the remaining non-zero weights is standardized to 1 to ensure unbiasedness (Deustch, 1996).

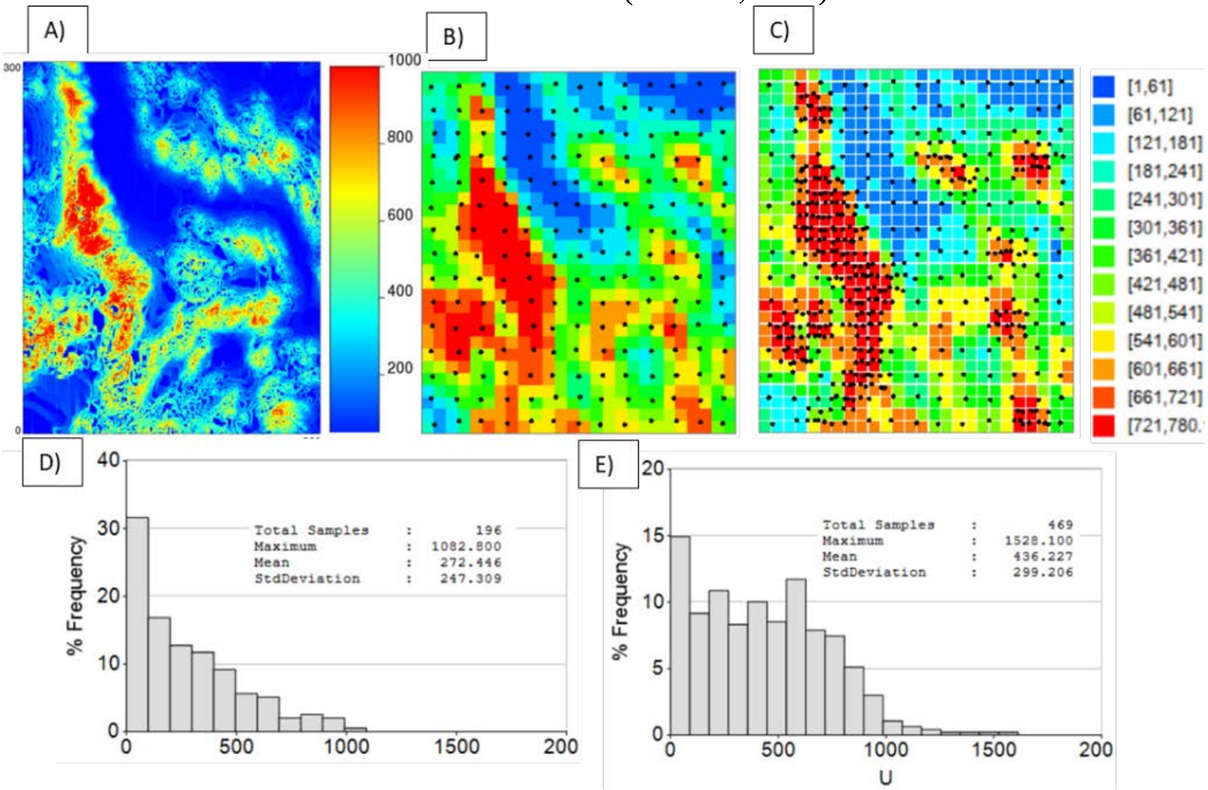

Figure 7 - Datasets and block models of U using the Walker Lake dataset: A) Exhaustive dataset; Block model 10 x 10 m estimated using rescaled datasets composed of B) 196 samples and C) 469 samples. The dataset histogram of D) 196 samples and, E) 469 samples.

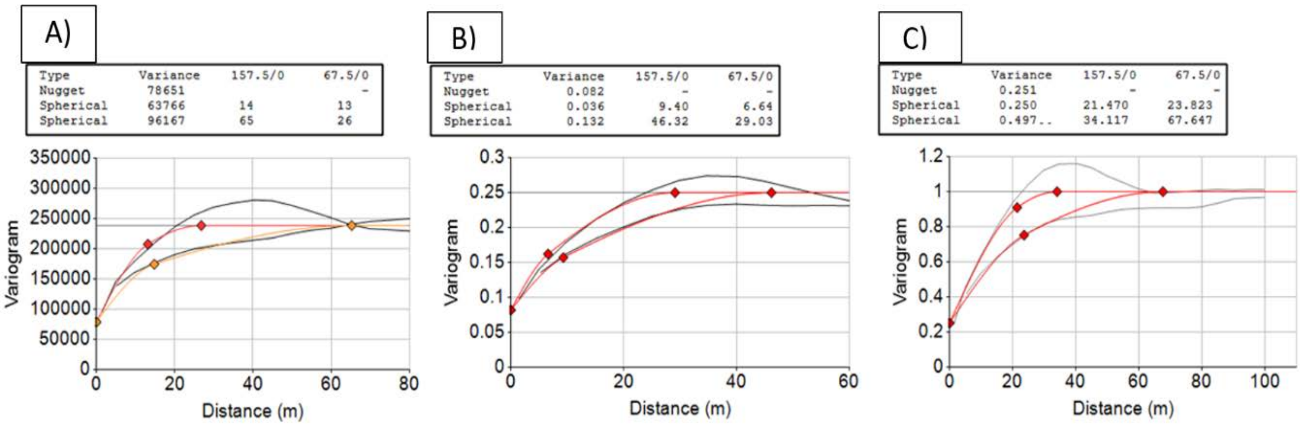

Figure 8 - Experimental variogram (Black line) and Variogram models (Red line) for variable U adjusted to data in A) Original units; B) Median indicator and, C) Normal-score units.

The comparison between methodologies is performed using two reference models:

- The "Actual Deviation" is the absolute difference between the grade of each reference value of each block the value estimated by OK using both re-scaled dataset (196 and 469 samples). The reference model is given by averaging into the 10 x 10 m block model the exhaustive dataset composed of 78.000 samples;
- Simulated Uncertainty assessed by Sequential Gaussian Simulation (SGS; Isaaks 1990; Deutsch & Journel, 1998). Each 10 x 10 m block was discretized into a 1 x 1 m grid and 100 realizations were performed at each one. The uncertainty associated with each block is given by the variance among its realizations.

To support our analysis, we fitted one linear model of regression to measure the similarity between the uncertainty estimated by each compared methods (x-axis) with both models of reference (y-axis).

The similarity is measured by: (i) the

coefficient of correlation “r”, which measures the relative percentage of the reference uncertainty variable variance that the model explains, ranging from 0 to 1; (ii) The standard error of the regression measures the average distance that the estimated uncertainty is from the regression line using ranked-value units. The analysis uses raw and ranked values. Rank regression provides an objective approach to dealing with non-normal distributions.

Next, the methods are experimentally compared to the Actual Deviation and the Simulated Uncertainty models using both rescaled datasets.

MEASURING THE MODEL UNCERTAINTY

All estimates were performed using the datasets composed of 196 and 469 samples. They used a search ellipse with distances equal to the ranges of their variograms (Figure 8), with a minimum of 12 and a maximum of 48 samples. It worth to highlight that the variable U is additive, then all methods were estimated at point support and the uncertainty obtained over a discretization of the 10 x 10 m block model:

- **Kriging Variance (KV):** KV computed from the OK estimates (Figure 7b and 7c);
- **Variance of Interpolation (IV):** Computed using both the kriging weights defined by OK;
- **Median IK:** The variable U distribution was discretized into 10 deciles and the indicator of each class was estimated using the Indicator Variogram of the median (Figure 8b). The order relation among classes was corrected by averaging the upward and downward corrections (Deutsch & Journel, 1998);
- **Combined Variance (CV):** Combination between KV and IV using Equation 2;
- **Combined Variance II (CVII):** Combination between KV and IV using Equation 5.
- **Multi-Gaussian Kriging (mGK):** Estimated using SK and the Normal-Score variogram (Figure 8c);
- **Combined Index (CI):** Combination between KV and mIK using Equation 4.

Table 1 present the coefficient of correlation and the error of regression between the reference and the compared models estimated using the both rescaled datasets. The best results are obtained by mGK, CI, mIK and CV, while KV correlation is negligible. The CVII overperformed the original CV in all the compared scenarios.

It is important to highlight that an unfair advantage is given to mGK when the simulated uncertainty is used as the refence model because many steps of the SGS and mGK workflows are shared, such as the same assumptions and theoretical background. The mGK is outperformed by CI and CVII when we analyze the “Actual Deviation”. The second point to discuss is the high performance of KV shown in Table 1.

Table 1 – Descriptive statistics between different estimates of uncertainty estimates using 196 or 469 samples and their association with two reference models: Uncertainty simulated by SGS; and the actual error between 10 x 10 m block models estimated by OK using the rescaled and the exhaustive dataset. The regression error is based on ranked values.

Estimates with 196 samples						
	Sim. Uncertainty			Actual Error		
Method	**r**	**r_{rank}**	**Reg. Error$_{rank}$**	**r**	**r_{rank}**	**Reg. Error$_{rank}$**
Krig. Var.	12%	11%	224	-3%	-3%	225
Interp. Var.	43%	37%	210	43%	38%	208
mGK	89%	91%	210	25%	36%	211
mIK	77%	84%	122	15%	38%	209
Comb. Var.	44%	38%	208	39%	37%	209
Comb. Var. II	75%	80%	136	40%	48%	198
Comb. Index	84%	88%	109	28%	44%	203
Estimates with 469 samples						
Method	**r**	**r_{rank}**	**Reg. Error$_{rank}$**	**r**	**r_{rank}**	**Reg. Error$_{rank}$**
Krig. Var.	12%	11%	224	-3%	-3%	225
Interp. Var.	43%	37%	210	43%	38%	208
mGK	89%	91%	210	25%	36%	211
mIK	77%	84%	122	15%	38%	209
Comb. Var.	44%	38%	208	39%	37%	209
Comb. Var. II	75%	80%	136	40%	48%	198
Comb. Index	84%	88%	109	28%	44%	203

Its performance may be attributed to the fact that the lowest-simulated uncertainty is coincident with the more densely-sampled areas.

Figure 9 shows the maps of uncertainty estimated by mGK, CVII and CI, the two reference models and their difference.

Estimated maps using the dataset of 196 samples have an uncertainty roughly correlated with the grade. The reason is that the high-grade and transition areas are spatially associated with samples with higher amplitude of variation.

The dataset with 469 samples partially balances the relationship between the sampling grid and local variability measured by mGK. In contrast, CVII and CI uncertainty maps still indicating association between higher uncertainty and high-grade areas, being these consistent with the "Actual Deviation" model of reference (Figure 9, right side).

Next, the results are discussed, and conclusions are drawn.

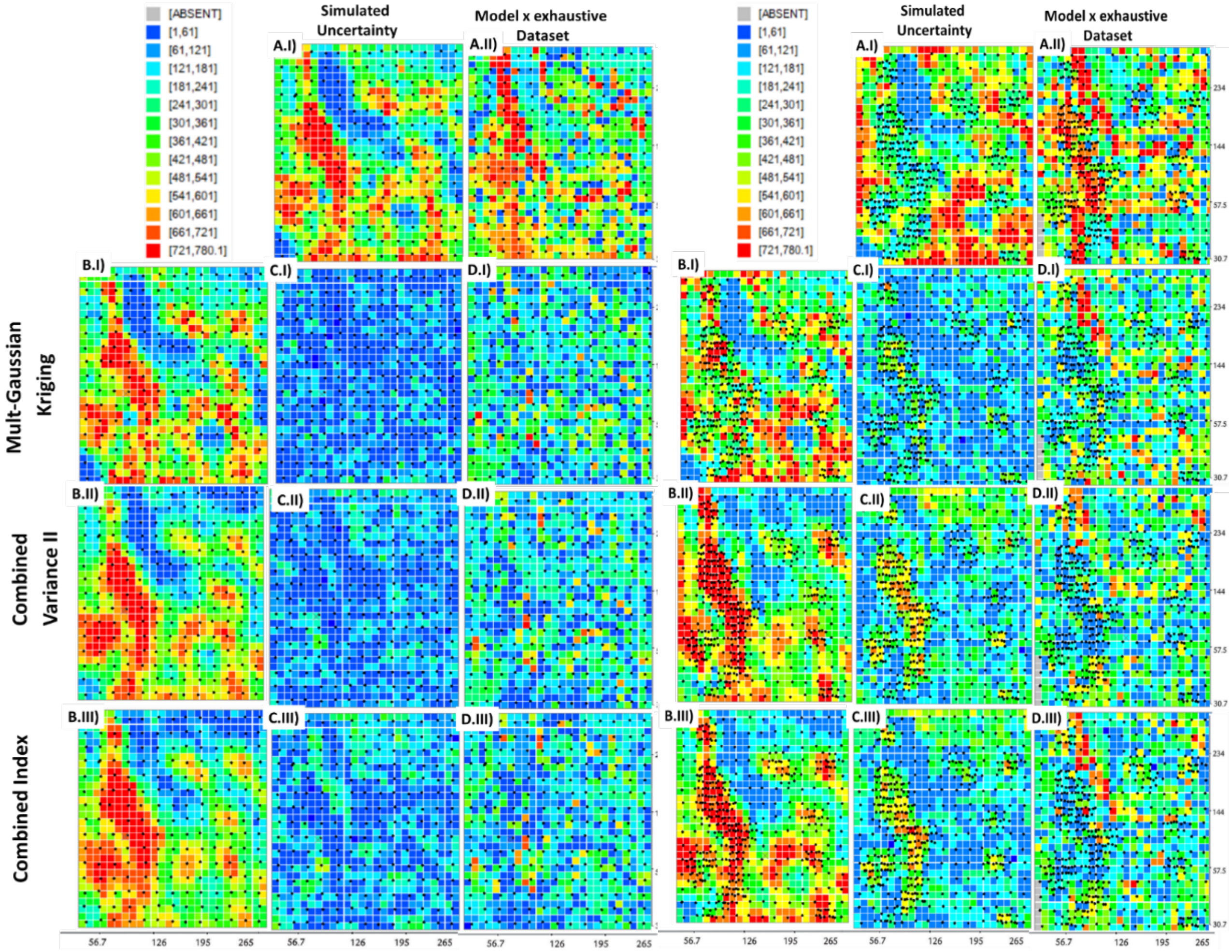

Figure 9 - Maps of reference generated by A.I) Geostatistical Simulation and A.II) the difference between the model estimated using the exhaustive and the samples with 196 and 469 samples in the left and hand-side hand, respectively. Uncertainty maps estimated using mGK (B.I), CVII (B.II) and CI (B.III) are shown and compared with both reference models by subtracting the ranked uncertainty value of each estimated and reference map (columns C and D).

DISCUSSIONS AND CONCLUSIONS

We proposed two methodologies to measure the uncertainty associated with kriging estimates. The Combined Index II combines the Kriging Variance, which is a good index of the data configuration, with the ccdf estimated by multiple Indicator Kriging. The second approach reviews the equation initially proposed by Arik (1999) to combine the Kriging Variance with the Interpolation Variance. In the presented case study, the proposed methodologies outperformed all other compared methods.

The proposed methodologies represent alternatives to the computationally intensive approach of stochastic simulation in some applications.

REFERENCES

ARIK, A. Uncertainty, Confidence Intervals and Resource Categorization: A Combined Variance Approach. **Proceedings**, ISGSM Symposium, Perth, Australia, 1999.

CANADIAN INSTITUTE OF MINING (CIM). **CIM Estimation of Mineral Resources and Mineral Reserves Best Practice Guidelines** Available in: https://mrmr.cim.org/media/1129/cim-mrmr-bp-guidelines_2019.pdf. Accessed in 02Feb2021, 2019.

CARVALHO, D. & DEUTSCH, C.V. An Overview of Multiple Indicator Kriging. In: J. L. DEUTSCH (Ed.), **Geostatistics Lessons**. Available in: http://geostatisticslessons.com/lessons/mikoverview. Acessed in 02Feb2021

DEUSTCH, C.V. Correcting for negative weights in ordinary kriging. **Computers and Geosciences** v. 22, n. 7, p. 765-773, 1996.

DEUTSCH, C.V. & JOURNEL, A.G. **GSLIB: Geostatistical software library and user's guide**: Oxford University Press, New York, 340 p., 1992.

GÓMEZ-HERNÁNDEZ, J.J.; SRIVASTAVA, R.M. One Step at a Time: The Origins of Sequential Simulation and Beyond. **Mathematical Geoscience**, v. 53, p. 193–209, 2021.

GOOVAERTS, P. **Geostatistics for Natural Resources Evaluation**. Applied Geostatistics Series. xiv + 483 p. New York, Oxford: Oxford University Press, 1997.

ISAAKS, E.H. A aplicação dos métodos de Monte Carlo à análise de dados espacialmente correlacionados: não publicado. Ph.D. tese, departamento de ciências da terra aplicadas, Stanford University, Stanford, Califórnia, 213 p., 1990.

ISAAKS, E.H.; SRIVASTAVA, R.M. **An introduction to applied geostatistics**: Oxford University Press, New York, 561 p., 1989.

JOURNEL, A.G. & HUIJBREGTS, C.J. **Mining geostatistics**: Academic Press, London, 600 p., 1978.

JOURNEL, A.G. Non-parametric estimation of spatial distributions. **Mathematical Geology**, v. 15, n. 3, p. 445–468, 1983.

MATHERON, G. Principles of Geostatistics. **Economic Geology**, v. 58, p. 1246-1266, 1963.

REMY, N.; BOUCHER, A.; WU, J. **Applied geostatistics with SGeMS: A user's guide**. Cambridge University Press, 2009.

VERLY, G. Grade control classification of ore and waste, a critical review of estimation and simulation based procedures. **Mathematical Geology,** v. 37, n. 5, p. 451–475, 2005.

VERLY, G. The multiGaussian approach and its applications to the estimation of local reserves. **Mathematical Geology,** v. 15, n. 2, p. 259-286, 1983.

YAMAMOTO, J.K. An alternative measure of the reliability of ordinary kriging estimates. **Mathematical Geology**, v. 32, n.4, p. 489-509, 2000.

Submetido em 2 de maio de 2021
Aceito para publicação em 28 de agosto de 2021